DISCLAIMER

This report was prepared as an account of work sponsored by an agency of the United States Government. Neither the United States Government nor any agency thereof, nor any of their employees, makes any warranty, express or implied, or assumes any legal liability or responsibility for the accuracy, completeness, or usefulness of any information, apparatus, product, or process disclosed, or represents that its use would not infringe privately owned rights. Reference herein to any specific commercial product, process, or service by trade name, trademark, manufacturer, or otherwise does not necessarily constitute or imply its endorsement, recommendation, or favoring by the United States Government or any agency thereof. The views and opinions of authors expressed herein do not necessarily state or reflect those of the United States Government or any agency thereof. Reference herein to any social initiative (including but not limited to Diversity, Equity, and Inclusion (DEI); Community Benefits Plans (CBP); Justice 40; etc.) is made by the Author independent of any current requirement by the United States Government and does not constitute or imply endorsement, recommendation, or support by the United States Government or any agency thereof.

SMALL-SCALE ASSESSMENT OF SIMPLIFIED CERAMIC WASTE FORM PROCESSING

Nuclear Fuel Cycle & Supply Chain

Prepared for
U.S. Department of Energy
Materials Recovery and Waste Form Development Campaign
J.E. Gesualdi, E. Schneiderlochner, Y. Liao, J. Rojas, and W.L. Ebert
Argonne National Laboratory

September 10, 2025
ANL/CFCT-25/15

ABSTRACT

The feasibility of directly processing glass-bonded sodalite ceramic waste form materials by heating a mixture of Zeolite 4A, chloride salt, and sodium borosilicate binder glass was demonstrated by generating laboratory-scale materials. This direct processing method eliminates pre-setting the moisture content of the Zeolite 4A, eliminates the step of occluding salt in the prepared Zeolite 4A prior to processing, and can be conducted using larger particle sizes of crushed Zeolite 4A and crushed borosilicate glass than those called for in the current method. These simplifications are expected to facilitate material transfer and handling in a hot cell or controlled atmosphere environment and be more readily implemented at large scale than the current method. Most materials made to assess these simplifications were directly processed at 925 °C for two hours in an argon atmosphere glovebox, but one material was processed at 925 °C for four hours and one material was processed at 880 °C for two hours. Sodalite was generated and became microencapsulated by the binder glass in all materials. The microstructures were uniform throughout each product, were similar in all products, and were similar to the microstructures of materials made previously using the pressureless consolidation or hot isostatic pressing methods. Various formulations showed the efficiency of sodalite generation was not sensitive to the salt-to-Zeolite 4A ratio or salt-to-glass mass ratio, although a greater relative mass of glass is required to encapsulate sodalite generated from large particles of aggregated Zeolite 4A. The upper limit of salt loadings that can be effectively processed remains to be determined. The effectiveness of direct processing provided new insights into the conversion mechanism. The salt was likely dissolved into the glass that transported NaCl into the Zeolite 4A aggregates and sodalite was generated in situ as NaCl migrated from the outside of the aggregate inward. Other salt cations (e.g., potassium, strontium, cesium, and probably lithium) remain dissolved in the glass encapsulating the zeolite/sodalite domains. When the glass solidifies during cooling, small halite inclusion phases form in glass within sodalite domains and large mixed salt inclusions form in glass surrounding the sodalite due to the low solubility of chloride in the (solid) glass. Other salt cations were oxidized during processing and formed inclusions in the bulk glass (e.g., neodymium). Initial degradation tests show the dissolution behavior of directly processed CWF (SCWF) materials is similar to CWF materials made using different methods.

THIS PAGE INTENTIONALLY LEFT BLANK

CONTENTS

FIGURES

TABLES

ACRONYMS AND ABBREVIATIONS

ACWF	Advanced sodalite Ceramic Waste Form
ANL	Argonne National Laboratory
ASTM	ASTM-International
BSE	Backscattered Electron (image)
BSG	Borosilicate Glass
CWF	Ceramic Waste Form
DOE	US Department of Energy
EDS	Energy-Dispersive X-ray Emission Spectroscopy
HIP	Hot Isostatic Pressing
INL	Idaho National Laboratory
MRWFD	Material Recovery & Waste Form Development (campaign)
NBS	Sodium Borosilicate (glass)
PC	Pressureless Consolidation
PNNL	Pacific Northwest National Laboratory
RH	Relative Humidity
SCWF	Simplified Ceramic Waste Form
SEI	Secondary Electron Image
SEM	Scanning Electron Microscope (or microscopy)
XRD	X-ray Diffraction

THIS PAGE INTENTIONALLY LEFT BLANK

ACKNOWLEDGEMENTS

This report was produced under the auspices of the US DOE Office of Nuclear Energy Nuclear Fuel Cycle & Supply Chain program Materials Recovery and Waste Form Development Campaign. Issuance of this report meets milestone M3FT-25AN030104016. Zeolite 4A materials were provided by Dr. Morgan Kropp and colleagues at the Idaho National Laboratory (INL) and NBS4 glass was provided by Dr. Brian Riley and colleagues at Pacific Northwest National Laboratory (PNNL). The ERX salt was synthesized by Dr. Levi Gardner (Argonne), XRD analysis was conducted by Dr. Sara Thomas (Argonne), and technical assistance was provided by Mr. Kyle Chamberlain and Mr. Joseph Azzaro (Argonne). Solution analyses were provided by Ms Yifen Tsai (Argonne Analytical Chemistry Laboratory) and are gratefully acknowledged.

This work was conducted at Argonne National Laboratory and supported by the U.S. Department of Energy, Office of Nuclear Energy, under Contract DE-AC02-06CH11357.

THIS PAGE INTENTIONALLY LEFT BLANK

MATERIALS RECOVERY & WASTE FORM DEVELOPMENT CAMPAIGN

Small-Scale Assessment of Simplified Ceramic Waste Form Processing

1. INTRODUCTION AND BACKGROUND

The glass-bonded sodalite ceramic waste form (CWF) was designed in the 1990's to accommodate chloride ions in salt waste within the crystal structure of synthetic sodalite ($Na_8[Al_6Si_6O_{24}]Cl_2$) that is then microencapsulated in a durable borosilicate glass matrix (see Ebert 2005 and references therein). The conversion of Zeolite 4A to sodalite occurs by reaction of NaCl in the salt with the reaction stoichiometry given in Equation 1.

$$\underset{\text{zeolite 4A}}{Na_{12}(AlSiO_4)_{12}} + 4NaCl \rightarrow 2\ \underset{\text{sodalite}}{Na_8(AlSiO_4)_6Cl_2} \quad (1)$$

The process developed to produce large-size CWF products that would fit in a standard DOE disposal canister from pyroprocessing salt waste is depicted in Figure 1. Process steps include crushing, milling, and sizing solid waste salt, crushing, milling, and sizing binder glass, and crushing, milling, sizing, and drying commercial Zeolite 4A. The sized salt and Zeolite 4A were mixed first at 500 ºC to occlude the salt within the cage structure of the zeolite with only a small amount of salt on the particle surfaces. The amount of so-called "free chloride" was measured to confirm the added salt was almost completely contained within the zeolite particles prior to processing. The salt-containing zeolite was then blended with sized glass frit and heated to at least 850 °C to process. Initially, the mixture was placed in a collapsable steel canister and processed by using hot isostatic pressing (HIP). It was later determined that pressurization was not necessary for effective stabilization. A pressureless consolidation method (referred to herein as the baseline PC method) was demonstrated to be suitable for processing mixtures of salt-containing zeolite and glass in a full-size DOE disposal canister and has been used since 2000 (Priebe and Bateman 2007).

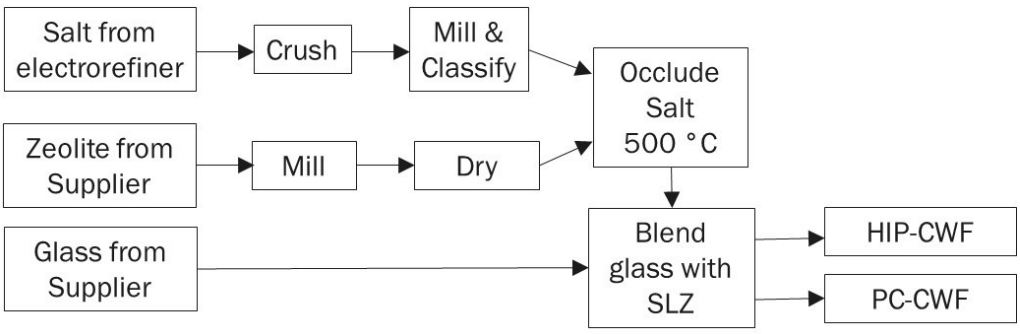

Figure 1. Flow diagram showing steps in baseline PC method for producing CWF.

Developmental research in the early 2000's demonstrated that (1) salt that had been occluded in the zeolite prior to processing migrated out of the zeolite framework and into the glass during processing, and (2) that some salt constituents (preferentially actinide and lanthanide elements) were oxidized by residual water in the zeolite during the occlusion process and decorated the surfaces of the aggregated particles (Ebert 2005). This suggested that, while the salt occlusion step provided control of the salt:zeolite stoichiometry, it was not necessary for the conversion reaction given in Eq. 1 to occur effectively. Further research demonstrated that the binder glass can be utilized to provide additional sodium to generate more sodalite to accommodate more chlorine and increase salt loading significantly (Ebert et al. 2017). It has been hypothesized that the production of CWF can be accomplished by simplifying the process depicted in Figure 1 without significantly decreasing the salt waste loading or waste form durability. Specifically, it has been hypothesized that the reagent size and dryness controls can be relaxed significantly to facilitate handling in a hot cell environment, that premixing to occlude salt in the Zeolite 4A pore structure is not necessary, and that the processing temperature can be decreased to 900 °C or lower (Ebert 2024).

2. EXPERIMENTAL APPROACH

The efficacy of using a simplified direct processing method is being assessed by synthesizing small-scale products and comparing the microstructure, density, and dissolution resistance (chemical durability) to materials having similar compositions that were made using HIP and PC methods with sized reagents and pre-occluded salt. Several materials were made using the simplified direct process to assess the effects of particle size, zeolite dryness, reagent mass ratios, processing thermal cycle (temperature and time), and conversion kinetics. Materials made using the simplified process are referred to as SCWF materials to distinguish them from materials made previously by using HIP or PC methods (e.g., Ebert 2005, Ebert et al. 2017). All SCWF materials were produced in a muffle furnace within an argon atmosphere glovebox near ambient pressure. Materials were made with a LiCl-KCl-based salt that is similar to salts used to make HIP CWF and PC CWF materials and represents salt waste recovered from the electrorefiner during pyroprocessing of sodium-bonded used nuclear fuel. All SCWF materials were made using Zeolite-4A that was provided by colleagues at the Idaho National Laboratory, NBS4[1] glass provided by colleagues at Pacific Northwest National Laboratory, and salt synthesized at Argonne.

2.1 Reagent Materials

Salt

The salt mixture referred to as "ERX" was formulated based on the waste salt composition expected after treatment of waste salt removed from the electrorefiner to recover remaining actinides and lanthanides (by electrolytic drawdown) and to recover and recycle a portion of the LiCl-KCl electrolyte (by salt crystallization). As listed in Table 1, the treated waste salt is dominated by sodium and active metal fission products (mostly Ba, Sr, and Cs). Although salt to be immobilized is expected to have very low rare earth element concentrations, a small amount of $NdCl_3$ was included in the ERX formulation to support comparisons with the elemental distributions observed in CWF made previously using PC and HIP methods.

Table 1. Composition of ERX salt, formula wt %

KCl	43	NaCl	13	$SrCl_2$	3
LiCl	34	CsCl	5	$NdCl_3$	2

The ERX salt was synthesized and prepared in a separate argon atmosphere glovebox with low oxygen and moisture contents to mitigate contamination prior to being incorporated into the SCWF materials. Appropriate masses (precision within 0.01 g) of dried pure reagent salts (99.5% pure or higher) were mechanically mixed in an Inconel crucible and heated to approximately 500 °C for eight hours in a furnace housed in an argon atmosphere glovebox maintained with < 10 ppm oxygen and < 1 ppm moisture. The salt was crushed and remelted to better homogenize.

The twice-solidified salt was crushed and sieved to isolate the +16, -16 +60 (1.2 – 0.25 mm), and -60 mesh size fractions. (Note: -16 means the particles passed through a 16 mesh sieve and +60 means the particles did not pass through a 60 mesh sieve.) Most SCWF materials were made using reagents sized -16 +60 mesh. The salt size for the baseline process is -30 mesh (<0.60 mm) for salt to be occluded in the Zeolite 4A particles prior to processing CWF with the HIP or PC method. The salt occlusion step is omitted in the conceptual simplified process being assessed, and molten salt is instead added directly to a heated mixture

[1] Note: NBS4 is an internal designation for a particular glass composition.

of Zeolite 4A and glass particles. Simulating the addition of molten salt during production of these initial SCWF materials was not deemed warranted until the product was determined to be acceptable. Devising a method to simulate the addition of molten salt is recommended for future development of the simplified process. Instead, crushed solid salt was mechanically mixed with Zeolite 4A and glass particles with the expectation that melted salt would coat the glass and Zeolite 4A particles rather than drain to the bottom of the crucible. The size of the crushed salt particles was selected to be similar to the size of the Zeolite 4A and glass particles to distribute salt grains uniformly throughout the mixture and detain the molten salt from draining during processing until reaction to generate sodalite occurred.

Binder Glass

The borosilicate glass NBS4 that was formulated to provide additional sodium for generating sodalite in what was referred to as advanced CWF (ACWF) materials made using the PC method was used to make the SCWF materials (Ebert et al. 2017). The composition of NBS4 is given in Table 2. About 200 g of NBS4 glass was provided by colleagues at PNNL. The NBS4 glass was crushed and sieved using a benchtop mill (IKA model A10) and vibratory sieve shaker (ATM Sonic Sifter) to isolate the -16 +30 (1.2 – 0.6 mm), +16, and -30 mesh size fractions. Most SCWF materials described herein were made using the -16 +30 mesh size fraction. The binder glass size called for in the baseline PC process is -60 +325 mesh (0.25 – 0.05 mm). The effectiveness of using coarser particle sizes of crushed glass to facilitate transfer and handling is being evaluated.

Table 2. Elemental composition of NBS4 glass, oxide mass percent

SiO_2	61.96%	Al_2O_3	4.20%	B_2O_3	6.30%
Na_2O	21.24%	CaO	4.20%	ZrO_2	2.10%

Zeolite 4A

Commercial Zeolite 4A beads are aggregates of ~5 μm crystallites that are held together with a proprietary clay binder. The mass of the binder is not distinguished from the mass of the Zeolite 4A crystallites in either formulations of SCWF materials or batching reagents. Some beads were crushed and sieved at INL to isolate the -4 +16 (4.75 - 1.20 mm) and -16 +30 (1.20 – 0.60 mm) mesh size fractions. These are both larger than the zeolite size of -60 +325 mesh (0.25 – 0.05 mm) called for in the baseline PC method. Both uncrushed beads and the -16 +30 mesh size fraction were provided by INL for the materials made at Argonne that are discussed herein. Additional materials were made at INL using the larger size fraction and uncrushed beads; those materials are not discussed in this report but will be the subject of future comparisons.

Both the whole beads and the crushed zeolite materials were preconditioned by equilibration at 48% relative humidity (RH) in a desiccator using a saturated solution of K_2CO_3 to fix the humidity at room temperature (approximately 23 °C). This ensures initial uniformity of residual water contents of Zeolite 4A used to make all SCWF materials at Argonne and INL. Samples of the humidity-equilibrated zeolite were preheated to different temperatures prior to use in tests to determine the effect of residual water on the conversion and characteristics of the product. It is expected that water will be evolved from the zeolite during heating and completely evaporate before the salt melts at approximately 400 °C. However, both the solid and molten salts are very hygroscopic and could absorb moisture released from the Zeolite 4A during processing. Also, heating the zeolite to higher temperatures could lead to a change in the crystal structure and affect interaction with the molten salt and the generation of sodalite. Characteristics of materials made with

Zeolite 4A that had been preheated to different temperatures or not preheated inform the need to control the water content of the source material prior to processing.

Additional materials were made using the as-received beads without crushing. The use of large zeolite beads provides insights into the kinetics of the conversion processes to generate sodalite and microencapsulate sodalite in glass. Larger size fractions of glass and salt were used to make the SCWF material with whole beads with the intent of assessing effects of the separation and settling of reagents during processing.

2.2 Reagent Material Characterization

Most materials were characterized by preparing polished cross sections and analyzing the surfaces using scanning electron microscopy. A Hitachi S-3400N scanning electron microscope (SEM) with an associated backscattered electron (BSE) detector and energy-dispersive X-ray emission spectrometer (EDS; Bruker) was used. Initial characterization included SEM/EDS to determine elemental composition and distribution. Secondary electron imaging (SEI) was used to highlight surface morphologies and BSE imaging was used to highlight and visually distinguish constituent phases having different compositions. Elements with higher atomic numbers scatter more efficiently than elements with lower atomic numbers and appear brighter in BSE images. Most SEM photomicrographs included in this report are of BSE images. Elemental phase compositions were measured by using both spot and small field of view analysis modes and the distributions of individual elements between different phases were visualized using EDS X-ray emission mapping.

A small number of crushed Zeolite 4A particles that had been equilibrated at 48% RH and then heated to 300 °C for 2 h were fixed in epoxy and a polished cross section prepared for SEM analysis. The photomicrograph in Figure 2a shows the bulk microstructures of a typical particle. The Zeolite 4A beads fracture into particles that are approximately spherical (rather than forming shards) and do not have visible fractures penetrating through the particles. The higher magnification image of the top right corner of the center particle in Figure 2b shows the presence of two major inclusion phases aggregated with spherical grains of Zeolite 4A that are less than 10 µm in diameter. The inclusion phase labeled 1 is enriched in calcium and magnesium and the inclusion phase labeled 2 is enriched in silicon and oxygen (likely SiO_2); neither sodium nor aluminum is detected in these inclusions. Similar inclusions were detected in many cross-sectioned particles. Some of the small spheroids of Zeolite 4A seen in Figures 2c and 2d appear fractured and puckered both before and after heating. This may indicate fracturing occurred during

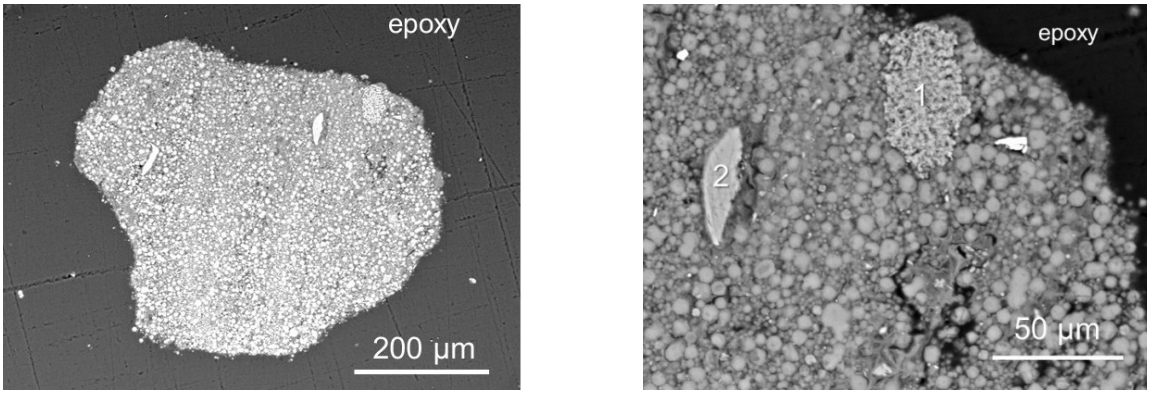

(a) (b)

Figure 2. (a) Cross section aggregate of Zeolite 4A, (b) embedded contaminants, and microstructure (c) before and (b) after heating at 300 °C.

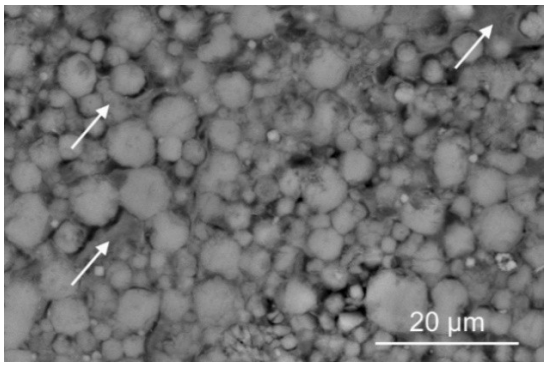

(c)

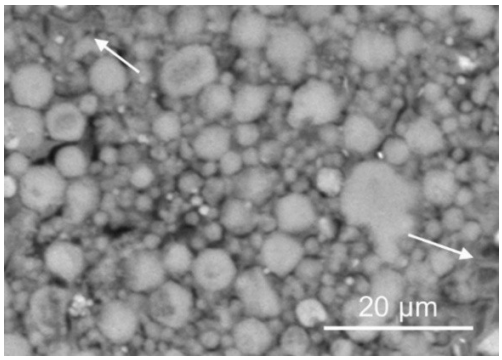

(d)

Figure 2. (cont.)

production of the reagent or during cutting and polishing of the cross section. Additional distortion of the individual particles may have occurred when the particles were heated. The arrows in Figure 2c and 2d point to amorphous features having the same appearance before and after heating, which may be clay binder.

Salt

Several pieces of crushed ERX salt were fixed in epoxy and a polished cross section prepared for SEM analysis. The cross section was prepared using absolute ethanol as the cutting and polishing fluid to minimize dissolution of the salt particles during preparation. The microstructure of a piece of crushed ERX salt is shown in the BSE images in Figures 3a and 3b. The flat edge in Figure 3a indicates the piece had been in contact with crucible when the salt was prepared. A cluster of lath-like strontium-bearing phases in the center of Figure 3b is embedded in a mixture of compositionally distinct phases with different contrasts in the BSE image. These indicate localized inhomogeneities on the millimeter scale had existed in the molten salt prior to freezing.

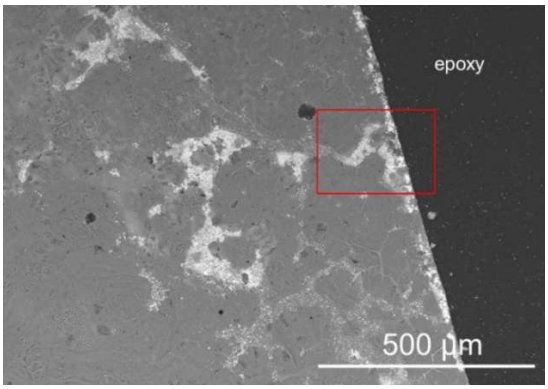

(a)

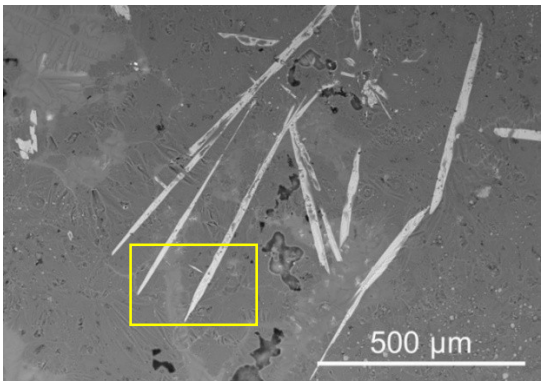

(b)

Figure 3. Photomicrographs of cross-section salt grains (a) from the outer edge and (b) from the interior of the cast salt ingot.

Figure 4 shows EDS X-ray maps of the field of view indicated by the red box shown in Figure 3a. These indicate the brightest regions are enriched in neodymium or strontium, which are likely mixtures of strontium and neodymium oxychlorides; various spot analyses in those regions measured 28-40 at% oxygen,

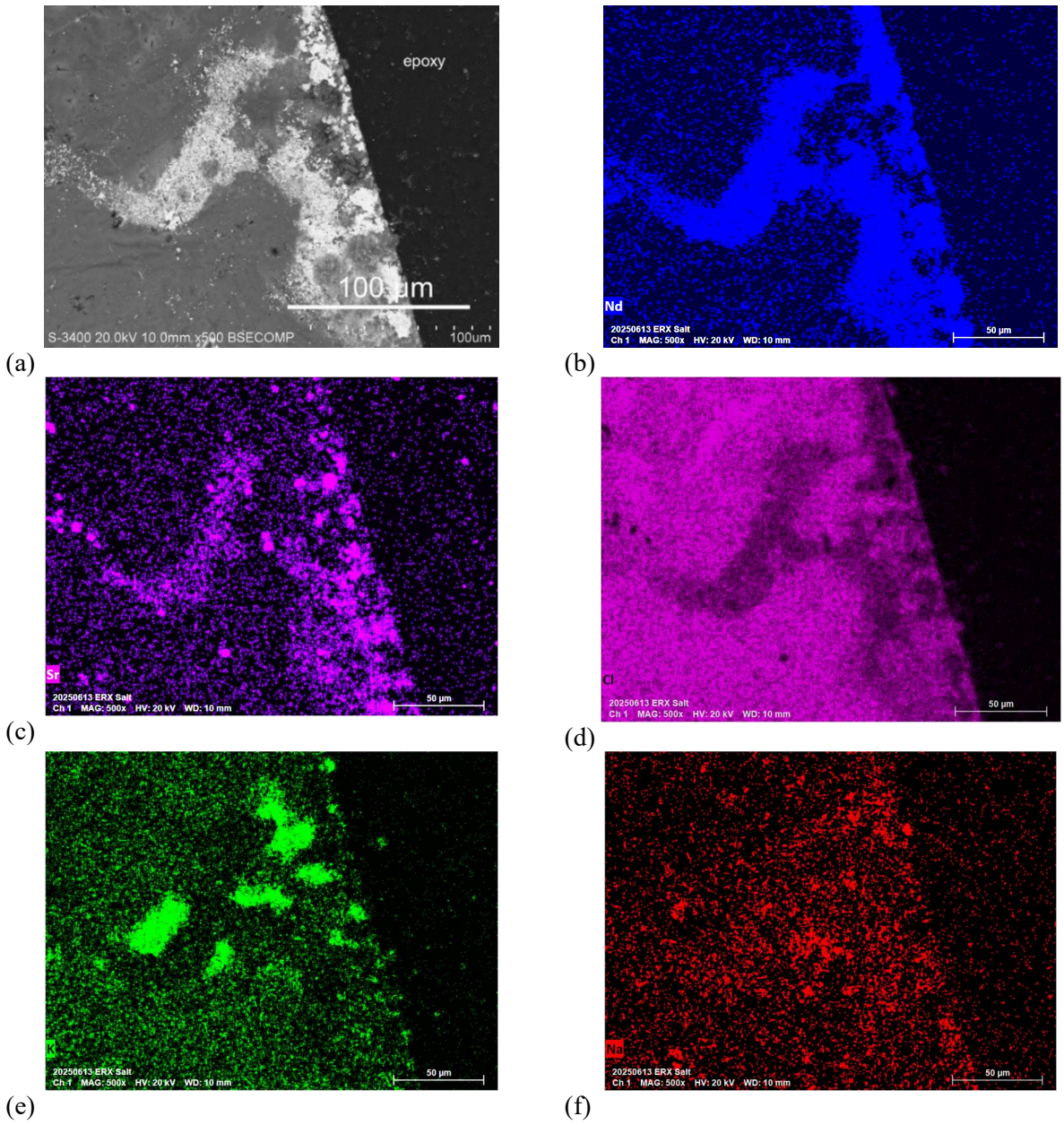

Figure 4. EDS X-ray elemental maps of region in salt grain: (a) photomicrograph of region and maps of (b) neodymium, (c) strontium, (d) chlorine, (e) potassium, and (f) sodium.

30-50 at% chlorine, 3-4 at% strontium, and 15-25 at% neodymium. The chlorine map shows higher chlorine contents in bulk salt surrounding the bright bands enriched in neodymium or strontium, and the distribution of potassium highlights the presence of compositionally distinct regions.

Figure 5 shows EDS X-ray maps of the field of view indicated by the yellow box shown in Figure 3b, which includes a cluster of $SrCl_2$ needles that formed within the bulk salt. The distributions of potassium and sodium indicate enrichment in different phases. The distribution of cesium also suggests segregation in the solidified salt, although the concentrations are low. When molten during processing, the salt is expected to be compositionally uniform, but phase separation occurs during solidification. Gram-sized additions of

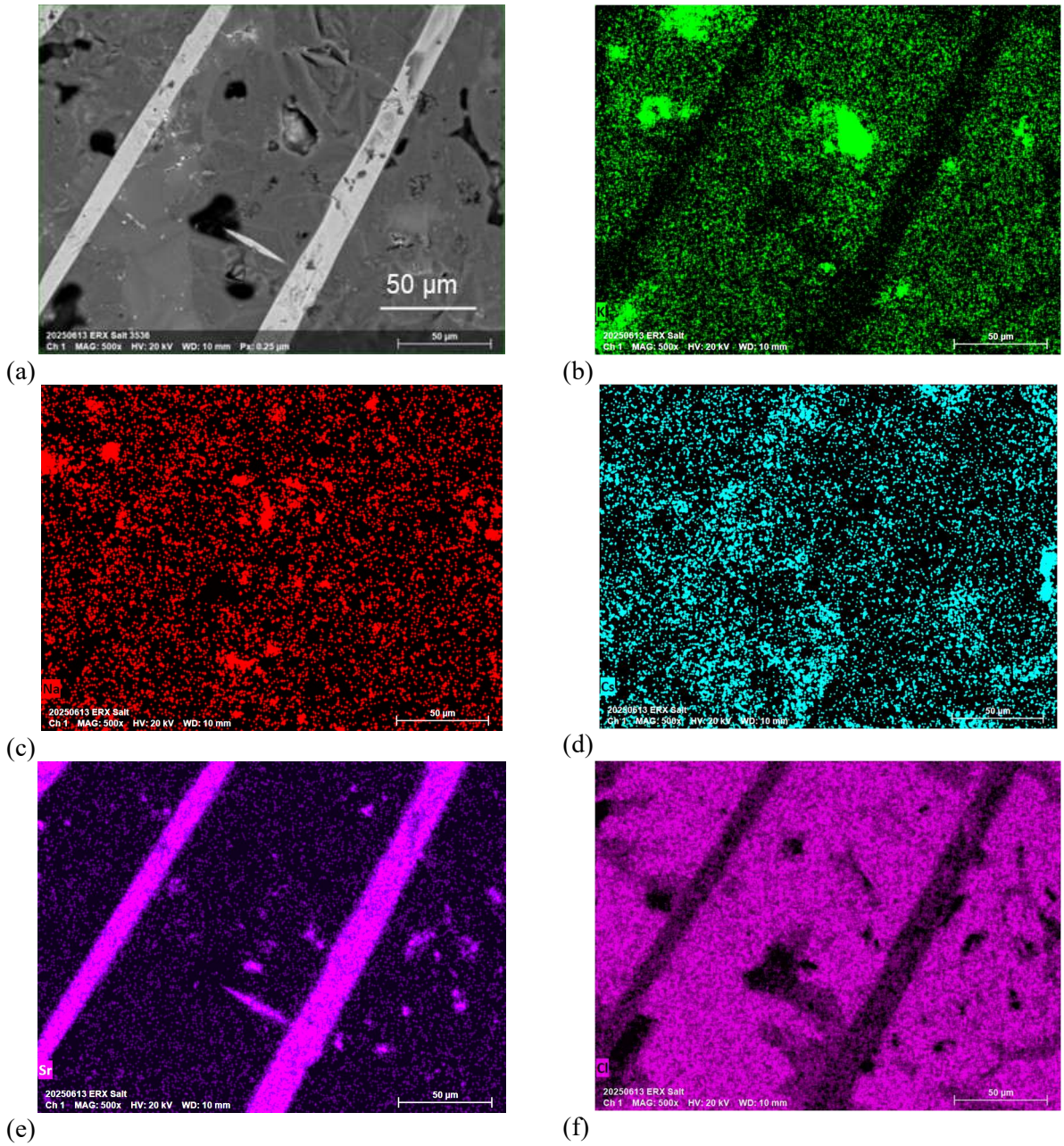

Figure 5. EDS X-ray maps of region in salt grain surrounding cluster of crystalline phases: (a) photomicrograph of region (b) potassium, (c) sodium, (d) cesium, (e) strontium, and (f) chlorine.

crushed reagent salt are expected to provide source salt compositions that are equivalent overall for production of all SCWF materials, although particles of crushed salt added as reagent will be compositionally distinct on the sub-millimeter scale and salt constituents may become localized when dissolved into the glass phase and during reaction with zeolite. The microstructure and composition of the solidified ERX salt can be compared to salt inclusions present in SCWF materials to determine if those inclusions are unreacted ERX salt, partially-reacted ERX salt, salt exsolved when the glass solidified, or halite formed as a by-product of the reactions with glass.

2.3 Material Synthesis

Materials were synthesized by mechanically mixing reagents in an alumina crucible (except SCWF-8 was made in a Type 304 stainless steel can) and heating in a muffle furnace housed in an argon atmosphere glovebox maintained with less than 100 ppm oxygen contamination. Heating ramps were typically 10 °C h^{-1} and the time required for heating (typically 90 minutes) is not included in the hold time at the target temperature of 880 °C or 925 °C used in the thermal cycle. The SCWF materials were made in the order listed in Table 3. A preliminary interaction test SCWF-0 was run to assess the interaction of molten salt with Zeolite 4A that had been preheated to evaporate some of the moisture and glass at a temperature slightly above the salt melting point. This was made to represent the first step of the thermal cycle used for SCWF-1. Materials SCWF-1 through SCWF-4 were made and compared to determine effects of the Zeolite 4A moisture content, heating cycle, and relative amount of glass. Material SCWF-1 was made using a two-step thermal cycle. The mixture was held one hour at 370 °C to melt and distribute the salt allowing time for salt to be absorbed into the zeolite microstructure, coat the zeolite and glass, or drain to the bottom of the crucible before increasing the temperature to 925 °C to melt the glass and generate sodalite. Materials SCWF-1 and SCWF-2 were both made using Zeolite 4A that had been heated to 100 °C to evaporate some of the moisture. Material SCWF-2 was made using the same mixture of reagents, but heated directly to 925 °C without a low temperature step to melt and distribute the salt. Material SCWF-3 was made using Zeolite 4A that was not preheated (i.e., had a high initial moisture content) and with a higher glass content, but using the same thermal cycle that had been used for SCWF-2. Material SCWF-4 was made using Zeolite 4A that had been dried at 300 °C to remove most moisture, but otherwise identical to SCWF-3. The microstructure of Material SCWF-4 was used as a basis of comparison to assess the effects of Zeolite 4A size, a lower processing temperature, the salt-to-Zeolite 4A mass ratio, and production in a steel canister. Material SCWF-5 was made using uncrushed Zeolite 4A that had been equilibrated at 48% RH and then heated at 300 °C to remove most of the moisture and with larger size fractions of salt and glass. Material SCWF-6 was made with reagents prepared the same as those used for SCWF-4, but was only heated to 880 °C rather than 925 °C for two hours. Material SCWF-7 was made with a higher salt-to-Zeolite 4A mass ratio than SCWF-4. Material SCWF-8 was made with a lower salt-to-Zeolite 4A mass ratio than SCWF-4, was processed in a Type 304 stainless steel can rather than an alumina crucible and had a lower total mass of reagents and product volume.

Table 3. List of SCWF materials produced[a]

SCWF ID	Salt	Zeolite		Salt/Zeolite	Glass	Salt/Glass	Thermal Cycle
	mass, g	mass, g	pre-treatment	mass ratio	mass, g	mass ratio	
SCWF-0	1.004	7.000	100 °C 2 h	0.143	2.012	0.499	370 °C 1 h
SCWF-1	1.002	7.004	100 °C 2 h	0.143	2.002	0.500	370 °C 1 h, 925 °C 4 h
SCWF-2	1.003	7.029	100 °C 2 h	0.143	2.036	0.493	925 °C 2 h
SCWF-3	0.751	5.250	none	0.143	4.001	0.188	925 °C 2 h
SCWF-4	0.753	5.251	300 °C 2 h	0.143	4.001	0.188	925 °C 2 h
SCWF-5[b]	0.752	5.251	300 °C 2 h	0.143	3.985	0.189	925 °C 2 h
SCWF-6	0.750	5.245	300 °C 2 h	0.143	4.000	0.188	880 °C 2 h
SCWF-7	0.909	5.094	300 °C 2 h	0.178	4.004	0.227	925 °C 2 h
SCWF-8[c]	0.250	2.333	300 °C 2 h	0.107	1.333	0.188	925 °C 2 h

[a] Made with -14 +60 mesh salt; -16 +60 mesh glass; -16 +30 mesh Zeolite 4A.
[b] Made with +14 mesh salt; +16 mesh glass; full-size Zeolite 4A beads.
[c] Processed in a Type 304 stainless steel can.

3. RESULTS AND DISCUSSION

3.1 Feasibility of Direct Processing

Materials SCWF-1, SCWF-2, SCWF-3, and SCWF-4 were made to demonstrate the feasibility of direct processing for comparison to materials made using the pressureless consolidation (PC CWF) method. The microstructures of Materials SCWF-1 and SCWF-2 were used to assess the behavior of molten salt during the thermal cycle: Material SCWF-1 was processed by first holding at approximately 370 °C for 1 h to melt the salt and provide time for the molten salt to either migrate into the zeolite grains or percolate to the bottom of the crucible (due to gravity), then heated to 925 °C for 4 h to generate sodalite. Material SCWF-2 was made using Zeolite 4A that had been heated at 100 °C prior to use to evaporate some of the water from the pores. Material SCWF-2 was heated directly to 925 °C and held for 2 h. A total mass of 0.851 g was lost during processing of Material SCWF-1 and 0.871 g during processing of Material SCWF-2. This is attributed primarily to evaporation of water from the Zeolite 4A (about 12% in both). In addition to moisture, a small amount of salt also evaporated. The microstructures of Materials SCWF-3 and SCWF-4 were used to assess the effect of drying the Zeolite 4A prior to processing: the Zeolite 4A used in SCWF-3 was not pre-heated and that used in SCWF-4 was heated to 300 °C before use. In addition, both SCWF-3 and SCWF-4 were made with lower salt contents and higher glass contents than what was used to make SCWF-1 and SCWF-2 to further assess the effect of the glass content on the abundance of large voids within the product. The mass losses during processing SCWF-3 and SCWF-4 were 1.199 g and 0.183 g (23% and 3%), respectively. The total mass loss during processing was clearly correlated with the moisture content of the Zeolite 4A reagents, but the moisture content did not affect the generation of sodalite or the product microstructure. Prior to synthesizing Material SCWF-1, a mixture of Zeolite 4A, salt, and glass equivalent to the mixture used for SCWF-1 was heated to 370 °C to determine how the melted salt become distributed (referred to as SCWF-0 in Table 3). Figure 6 shows the mixed Zeolite 4A and glass particles, salt added on top of the mixture (but not mixed with the zeolite and glass) before heating, and the surface after heating. It appears that most of the salt remained on the surface during heating; some Zeolite 4A particles look shiny amber and to be coated with salt, though most of the salt appears to have retained the light turquoise color. It can be seen that the salt neither percolated to the bottom nor become distributed between particles. It is likely phase separation occurred after heating to above the solidus temperature of the salt (see Section 2.2). This indicates the hold to melt and distribute salt is not necessary in the thermal cycle used to synthesize the SCWF materials.

(a) (b) (c)

Figure 6. Top view of particles of (a) Zeolite 4A and glass mixed in an alumina crucible, (b) salt added over Zeolite 4A and glass mixture before heating, and (c) surface after heating to 370 °C for 1 hour.

The SCWF materials were made by adding weighed amounts of Zeolite 4A, NBS4 glass, and ERX salt into an alumina crucible within an argon atmosphere glove box. The three reagents were mechanically mixed to distribute uniformly by stirring with a spatula. The crucible was placed in a muffle furnace housed in the glove box that was flushed with ultrapure argon and processed following the imposed thermal cycle then furnace cooled. Reagents added to an alumina crucible are shown in Figures 7a and 7b before and after mixing. The product is shown in Figure 7c. The material densified to about half the volume occupied by the mixture of reagents and shrunk away from the crucible sides, although a few particles remained stuck to the inside of the crucible. Some SCWF products were removed from the crucible for analysis, but in most cases, epoxy was added directly to the crucible to stabilize the product for cross sectioning.

(a) (b) (c)

Figure 7. Photographs of (a) reagents added to alumina crucible, (b) stirred reagents, and (c) processed SCWF material.

Optical photographs and SEM photomicrographs of SCWF-1, SCWF-2, SCWF-3, and SCWF-4 products are shown in Figure 8. Cross-sectioned Materials SCWF-1 and SCWF-2 have very similar visual appearances and microstructures. The appearances of cross-sectioned Materials SCWF-3 and SCWF-4 are similar to each other, but the sodalite domains in both materials appear more completely encapsulated by glass than the sodalite domains in Materials SCWF-1 or SCWF-2, which were made with a smaller amount of glass. Sodalite was generated and microencapsulated by glass in all four materials. Encapsulation of sodalite domains are shown in Figures 8c and 8d and encapsulation of individual sodalite grains with a sodalite domain is seen in the high magnification photomicrograph on the right side of Figure 8b. The

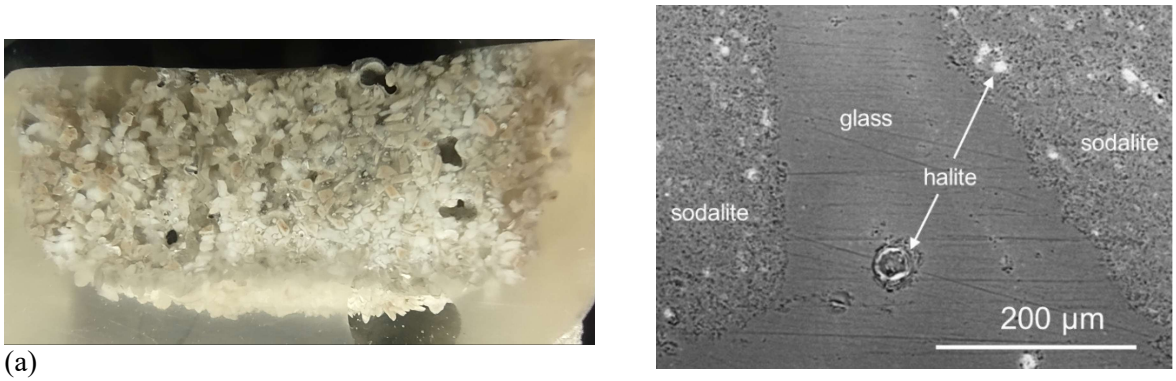

(a)

Figure 8. Optical photos and SEM photomicrographs of SCWF materials showing generation of sodalite microencapsulated in glass: (a) SCWF-1, (b) SCWF-2, (c) SCWF-3, and (d) SCWF-4.

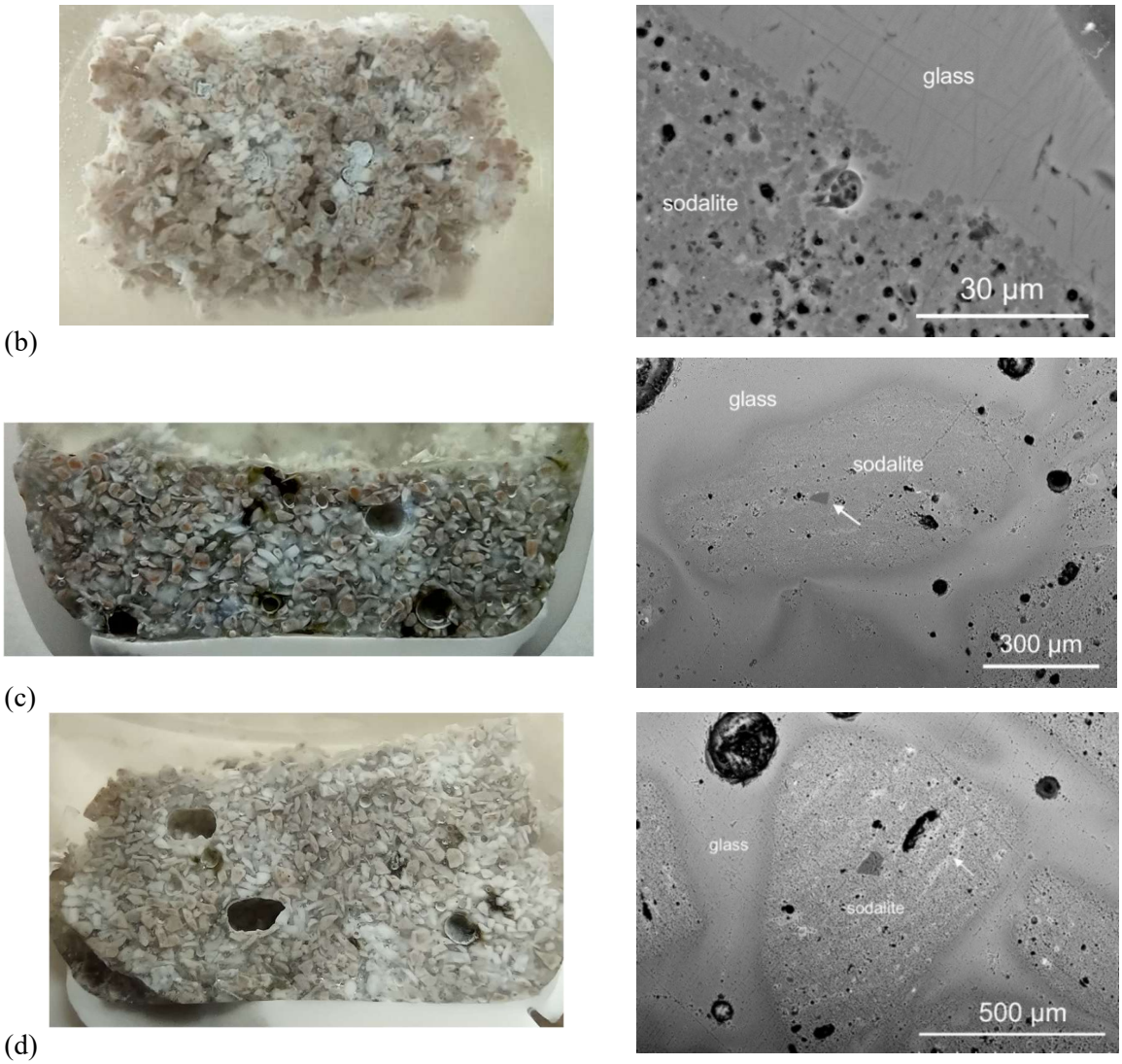

Figure 8. (cont.)

individual sodalite particles appear darker than the surrounding glass and micropores are darkest. Note that the electron backscattering properties of sodalite and the glass are similar and sodalite domains are readily recognizable in lower magnification images due to the microporosity. The halite inclusions have brighter contrast in backscattered electron images due to the higher atomic number of chlorine compared to the other elements present in the sodalite and glass. Phases containing elements having higher atomic numbers than chlorine (e.g., strontium and neodymium) are brighter (e.g., see Figure 4a), but those phases are not present in these fields of view. Note that silica contaminants in particles of Zeolite 4A remained within the sodalite domains that formed, as that located by the arrow in Figure 8c in SCWF-3.

Figure 9 shows a region of SCWF-1 with a relatively large pore partially filled with salt and polishing debris surrounded by glass and sodalite domains. The sizes of the sodalite domains are consistent with the -30 +60 (0.6 – 0.25 mm) size fraction of crushed Zeolite 4A. Likewise, the size of the salt-filled void in the center of the photomicrograph is consistent with the particle size range of the reagent salt. As discussed below, the composition of salt in that void and other inclusions differs from the composition of the reagent ERX salt. Many halite salt inclusions are seen to have been generated within the sodalite domains.

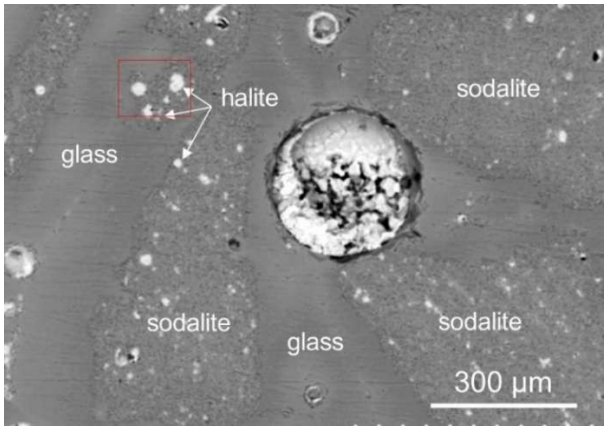

Figure 9. Region of SCWF-1 with a large inclusion of incompletely reacted salt in the glass phase and small inclusions of by-product halite in sodalite domains.

Elemental EDS X-ray maps of the area shown in Figure 9 are provided in Figure 10. The distribution of chlorine highlights the presence of halite inclusions in the sodalite domains. Sodium is more abundant in the sodalite domains than in the surrounding glass, but potassium is more abundant in the glass than in sodalite. Some potassium is also detected with sodium and chlorine in the large inclusion.

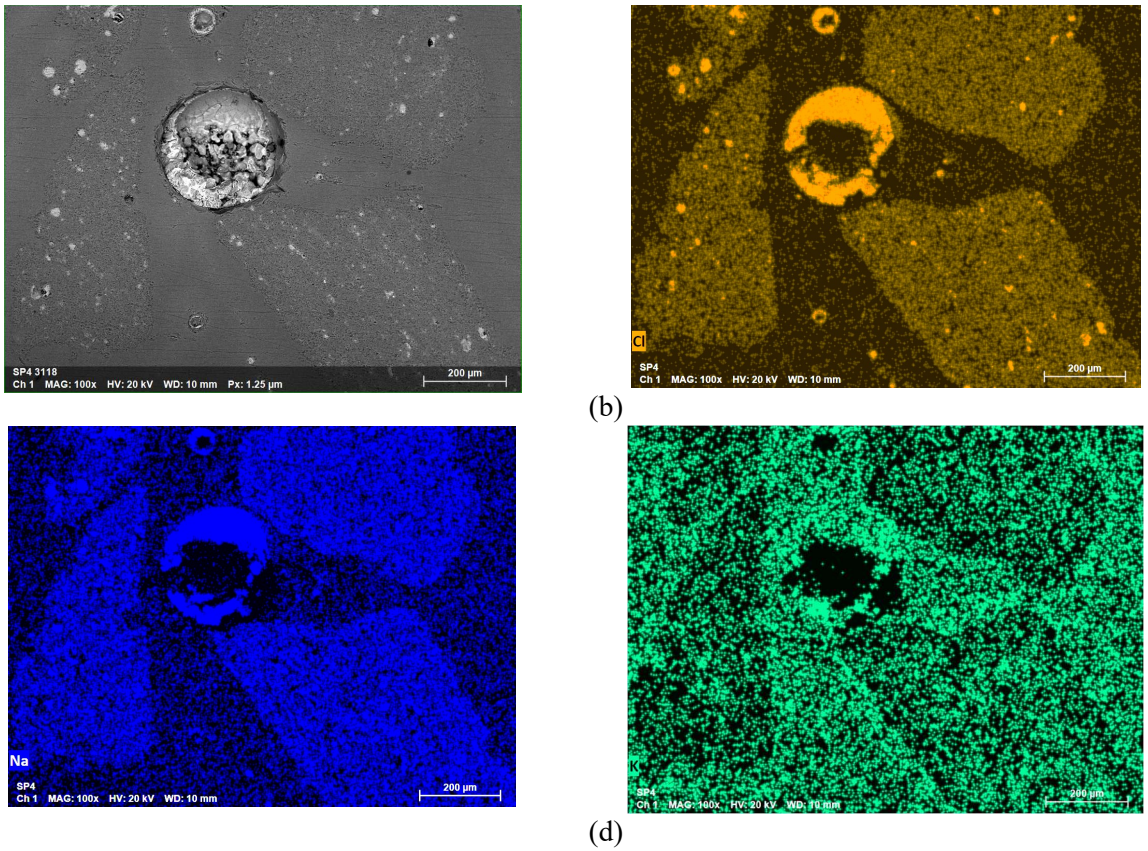

Figure 10. Microstructure of region of SCWF-1 (a) photomicrograph and EDS X-ray maps of (b) chlorine, (c) sodium, and (d) potassium.

A high magnification image of the field of view in the red box in Figure 9 is shown in Figure 11 with elemental EDS X-ray maps showing several halite inclusions formed within a sodalite domain. Potassium (and probably lithium; EDS is not sensitive to lithium) from the reagent salt is dissolved in the glass but is not detected in the halite phases. The sodium concentration is highest in the halite and higher in the sodalite grains than in either the bulk glass or in glass between the sodalite grains.

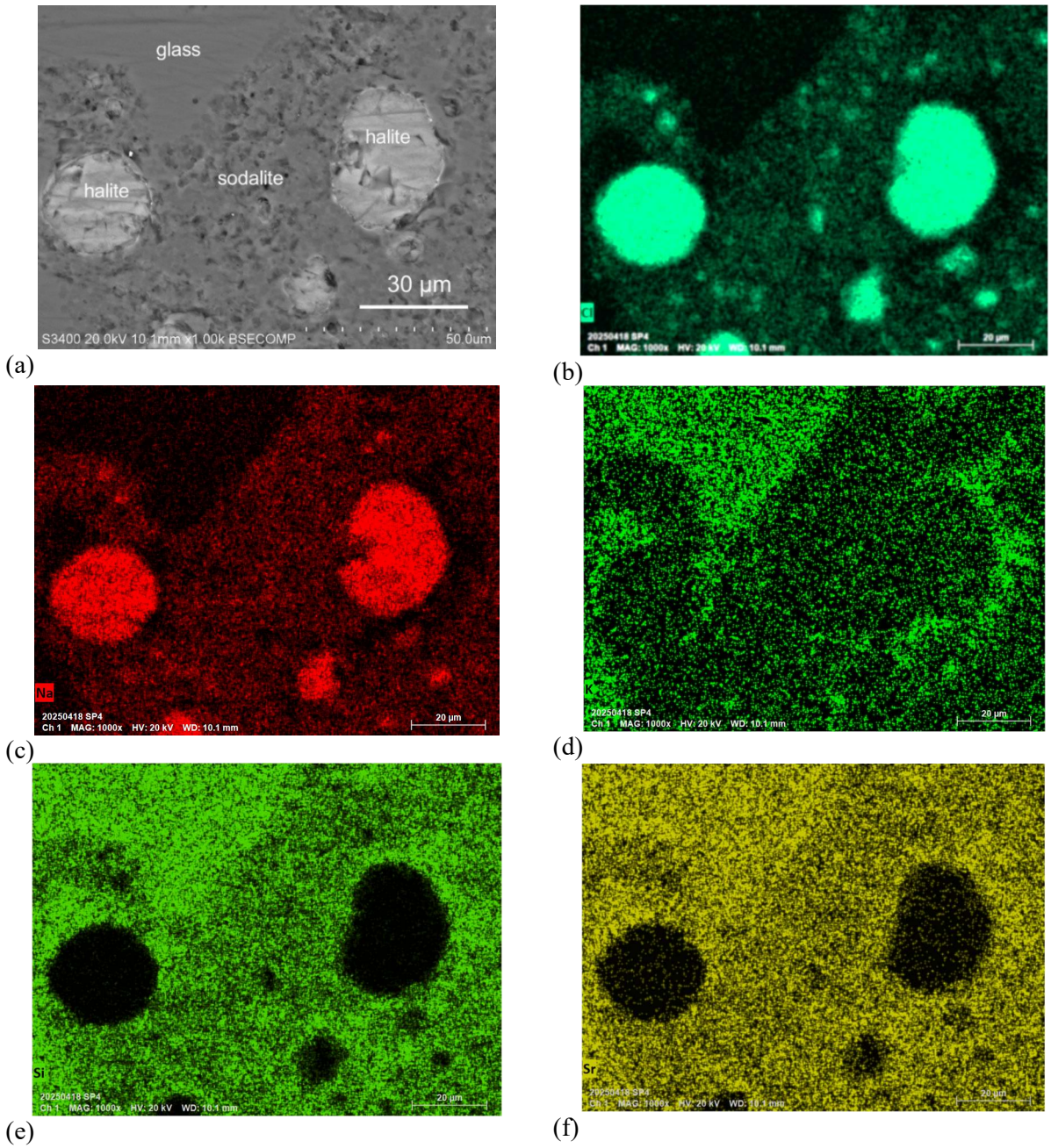

Figure 11. Microstructure of SCWF-1 (a) photomicrograph and EDS X-ray maps of (b) chlorine, (c) sodium, (d) potassium, (e) silicon, and (f) oxygen.

Material SCWF-4 was used as a reference material for measuring processing effects that are discussed in Section 3.2. Material from approximately one-half of the SCWF-4 product was crushed and analyzed by using X-ray diffraction (XRD) to confirm the identities of constituent crystalline phases. The measured XRD pattern is shown in Figure 12 with lines drawn to represent reference peaks for Zeolite 4A, sodalite (37-0476), nepheline (35-0424; major peaks) and halite (05-0628). The measured pattern is consistent with sodalite and a small amount of halite, but does not have peaks corresponding to either Zeolite 4A or nepheline. High resolution plots of neighboring halite and sodalite peaks are shown in Figure 13.

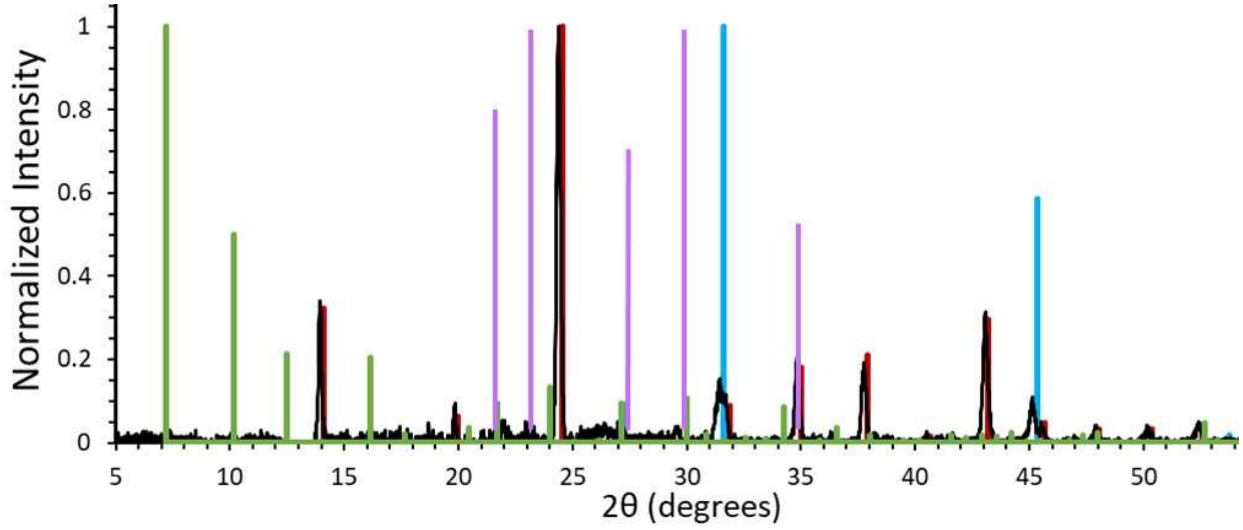

Figure 12. XRD pattern of pulverized SCWF-4 (black) overlaid with standard peak locations and relative intensities for Zeolite 4A (green), sodalite (red), nepheline (purple), and halite (blue).

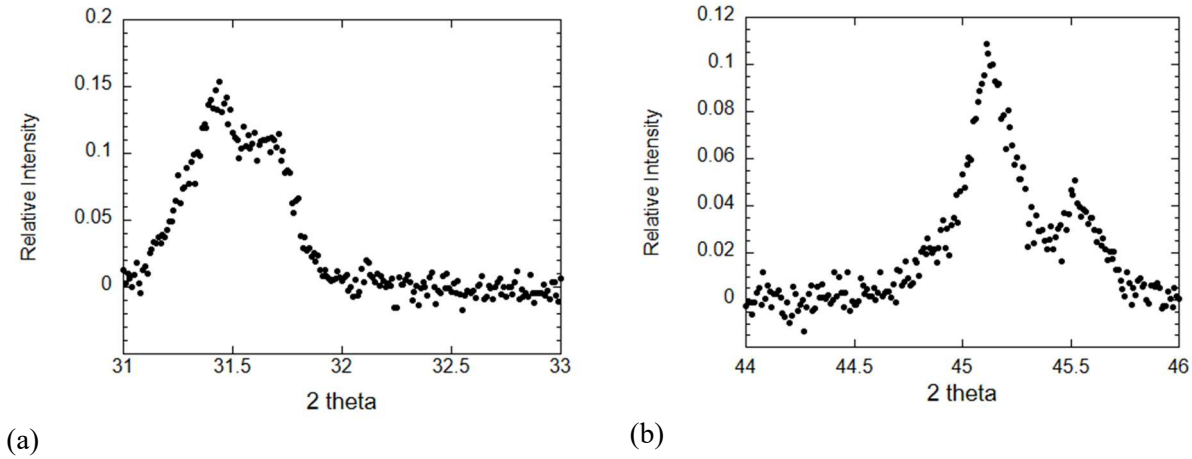

(a) (b)

Figure 13. High resolution plots of XRD patterns near neighboring halite and sodalite peaks (a) at 31.5° and (b) at 45.1°.

All of the crushed zeolite used to make the first four SCWF materials was converted to sodalite during the thermal cycle that was used. Four additional materials were made to measure the effects of the Zeolite 4A particle size, salt:Zeolite 4A ratio, and measure interaction with a steel canister.

3.2 Conversion Processes

Zeolite Size

Material SCWF-5 was made with the same masses of Zeolite 4A, salt, and glass as used to make SCWF-4 and under the same conditions as SCWF-4, except full-size beads of Zeolite 4A were used instead of crushed material to determine the nature and extent of conversion. The zeolite beads were pre-equilibrated at 48% RH and then heated at 300 °C for 2 h, the same pre-treatment as the crushed zeolite used to make SCWF-4. Larger pieces of salt and glass were used than in previously synthesized SCWF materials with the intent of mitigating salt drainage through the larger gaps between particles during processing. Figure 14a is a top view photograph of the product material in the crucible. The larger lighter-colored spheres at the top surface seen on the right-hand side appear unreacted and the darker-colored beads lower in the vessel appear to be smaller, coated with glass, and reacted. Epoxy was added to fix the beads and the crucible was cut as indicated by the dashed line to prepare the cross section. Figure 14b shows the bottom half of the cross-section. Only beads near the bottom of the crucible have been fully embedded in glass. The glass is difficult to distinguish from epoxy due to similar contrast in the photograph (it is most visible on the right-hand side about half-way up), but the glass is about half-way up the pile of beads. At least twice the amount of glass (i.e., 8 g glass for 5.3 g zeolite) would be required to completely encapsulate these large-size beads due to inefficient packing density. Layers of sodalite are evident surrounding remaining zeolite cores of the encapsulated beads. The thickness of the outer layer on different beads varies because individual beads were cross-sectioned to different depths (i.e., most cross sections are not at the full diameter). The cross sectioned cores of several beads show porosity and nearly concentric voids that are likely residual features from when they were manufactured.

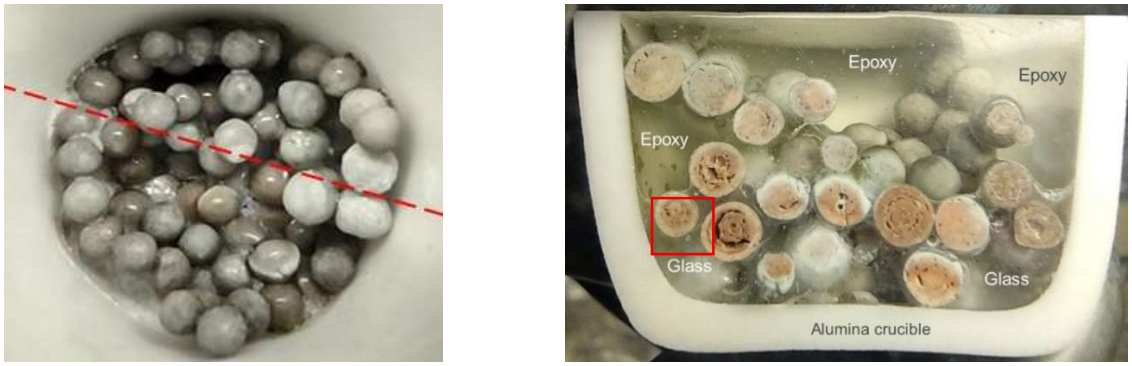

(a) (b)

Figure 14. Photographs of material SCWF-5 (a) view of surface in crucible and (b) polished cross section of product fixed in epoxy.

Figure 15 shows a high magnification image and EDS X-ray maps of the bead indicated by the red square in Figure 14b, which is near the top of the glass level. The formation of a layer of sodalite due to reaction of Zeolite 4A with salt (in the presence of glass) is most clearly indicated by the chlorine and sodium maps: sodalite contains chlorine and more sodium than does Zeolite 4A. The presence of chlorine reveals that Zeolite 4A has been converted to sodalite. That the chlorine map is slightly brighter in the zeolite core region than in the glass regions is likely an artifact of the measurement, such as background responses of the two materials, but may indicate that salt penetrated deeper into the zeolite core than what appears to the conversion reaction front. Lithium is not detected by EDS and LiCl may have migrated throughout the zeolite volume. The silicon and aluminum contents of Zeolite 4A and sodalite are very similar and do not

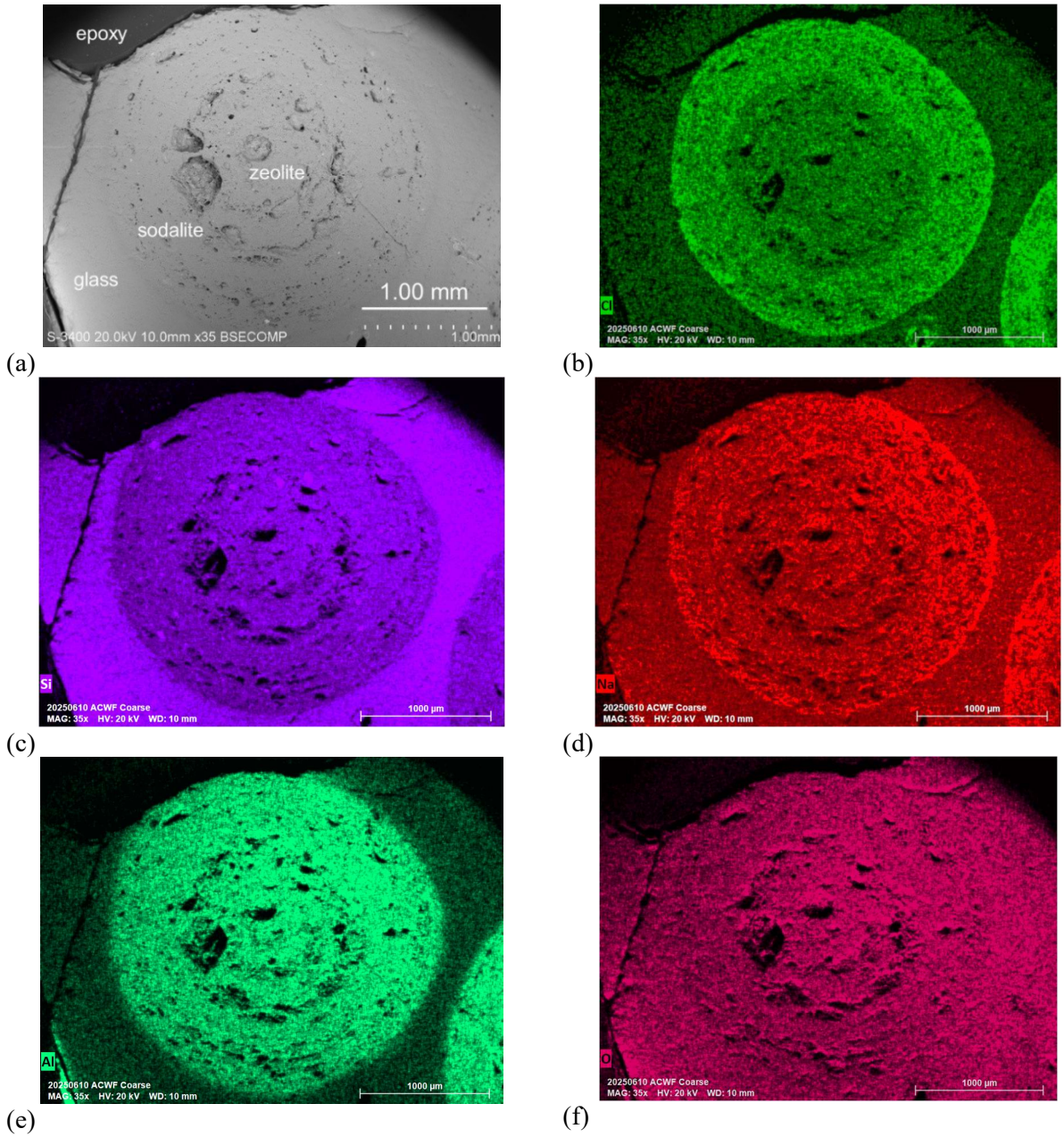

Figure 15. Microstructure of region of SCWF-5 (a) photomicrograph and EDS X-ray maps of (b) chlorine, (c) silicon, (d) sodium, (e) aluminum, and (f) oxygen.

distinguish between the two phases, but the silicon content of the glass is higher in either Zeolite 4A or sodalite and the aluminum content of the glass is lower than in both those phases. The oxygen contents of the glass, Zeolite 4A, and sodalite phases are all very similar. It is instructive to note that beads near the top of the glass level have visible outer shells of sodalite, which means they were penetrated by salt. The salt melted at approximately 400 °C whereas NBS4 glass became fluid at higher than approximately 800 °C. The extent of sodalite generation indicates the salt becomes fairly uniformly mixed with the molten glass during processing. The thicknesses of altered layers on beads that were cross sectioned nearly in half indicate the conversion rate under these processing conditions. The thickness of the chlorine shell in

Figure 15b generated during the two hours of processing is approximately 400 µm. That bead was not cut exactly in half so the imaged layer is not perpendicular to the surface of the bead. Nevertheless, it provides an upper limit to the conversion rate of 200 µm h^{-1}. The microstructures of other SCWF materials that were made with crushed Zeolite 4A particles larger than 30 mesh (>0.6 mm) indicated those particles were completely converted to sodalite within two hours of processing, which indicates an average penetration rate of >150 µm h^{-1}.

Lowered Processing Temperature

Material SCWF-6 was processed at 880 °C, which is approximately 30 °C higher than the temperature believed to be required for sodalite generation. The relative amounts of salt, Zeolite 4A, and glass closely matched those used to make material SCWF-2 by processing at 925 °C. Cross sections of both materials are shown in Figure 16 for direct comparison. The macrostructures and microstructures of the two materials are very similar and the Zeolite 4A particles were completely converted to sodalite in both materials.

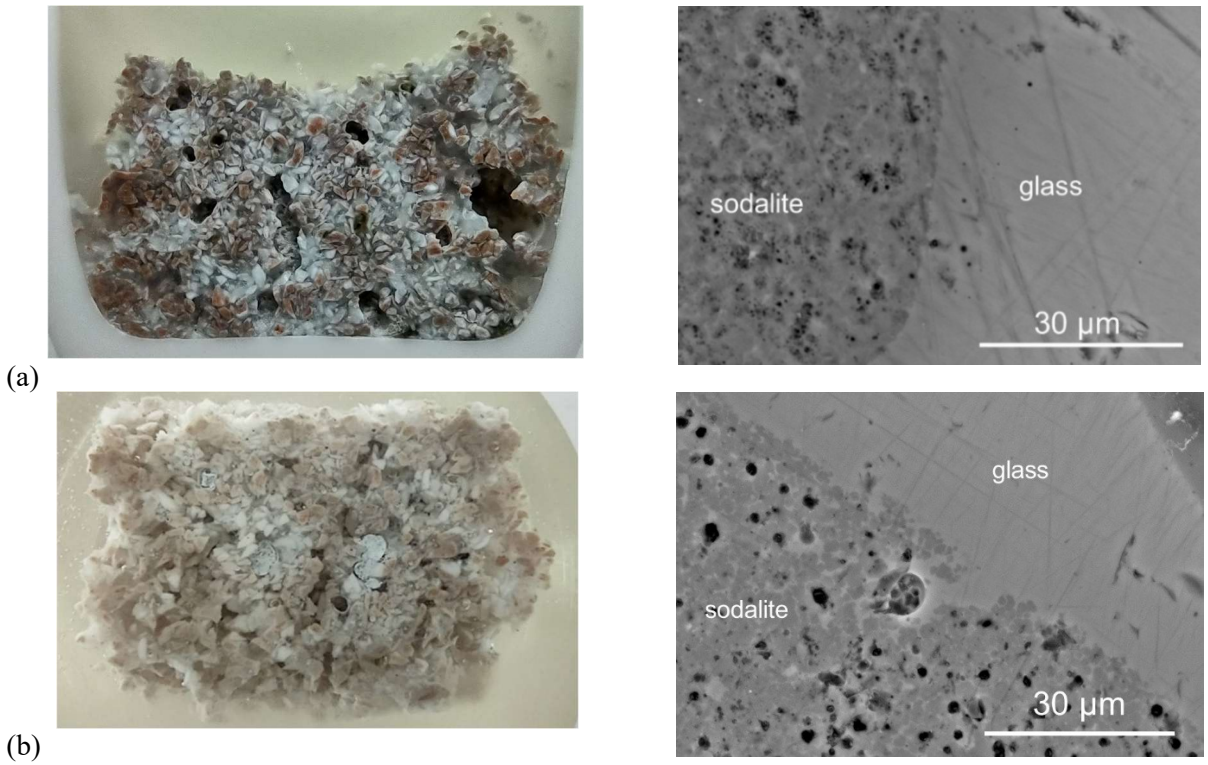

Figure 16. Photograph and microstructure of region (a) of SCWF-6 processed at 880 °C and (b) SCWF-2 processed at 925 °C.

A higher magnification image of a representative area in SCWF-6 and EDS X-ray maps for several elements are shown in Figure 17. The clusters of bright features in the center-right are Nd_2O_3 crystals encapsulated in the glass (note the absence of chlorine signal in that area). Potassium from the salt has been distributed throughout the glass. Calcium in the NBS4 glass remained in the glass phase of SCWF-6 and magnesium contaminants in the Zeolite 4A remained in the sodalite domains.

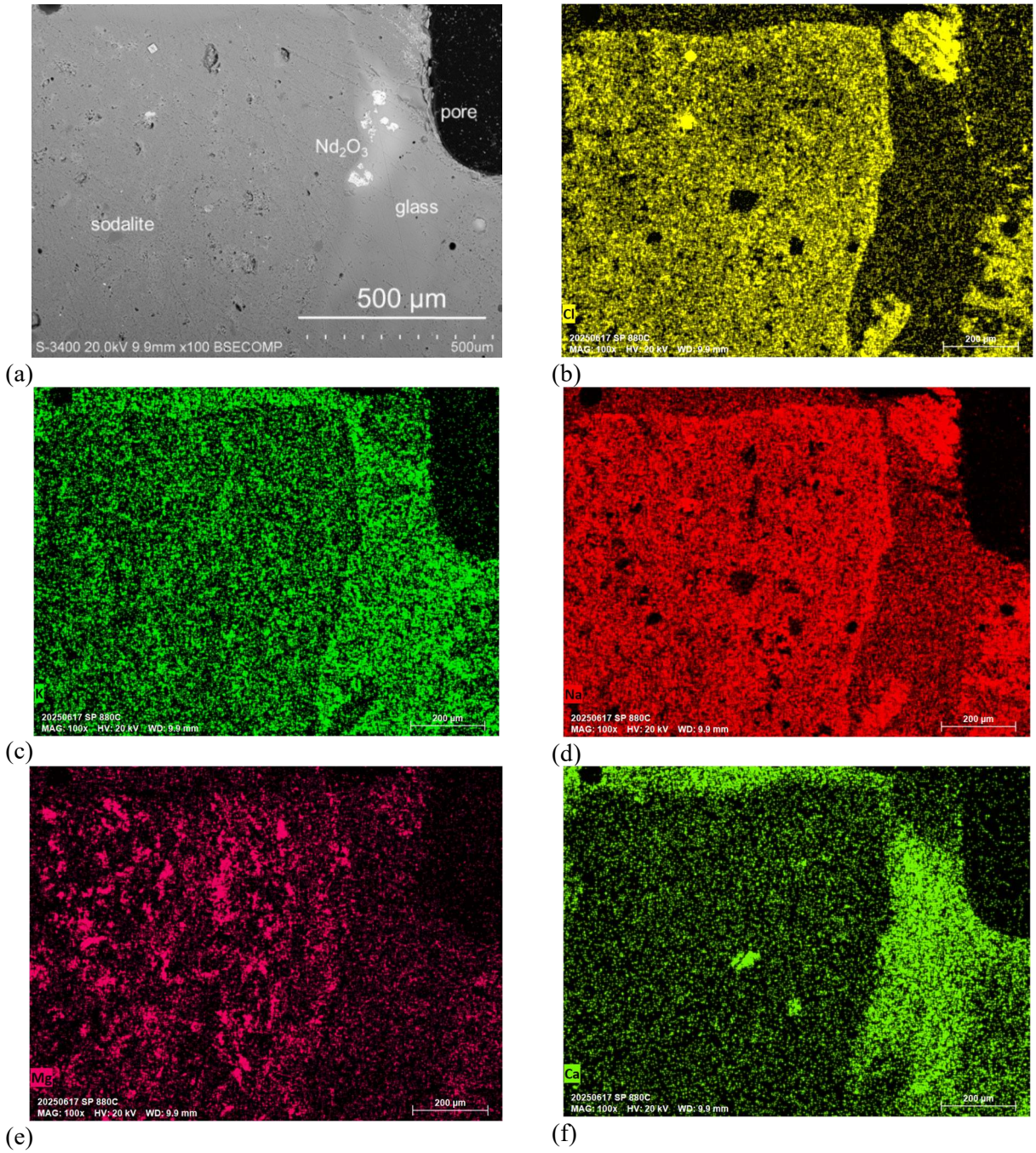

Figure 17. Microstructure of SCWF-6 (a) photomicrograph and EDS X-ray maps of (b) chlorine, (c) potassium, (d) sodium, (e) magnesium, and (f) calcium.

Increased Salt Content

Material SCWF-7 was made under the same conditions as SCWF-4, but with a higher salt:Zeolite 4A mass ratio. The 4:1 stoichiometry of Equation 1 (NaCl:Zeolite 4A) corresponds to a mass ratio near 1:7 based on the chloride content. A superstoichiometric salt:Zeolite 4A mass ratio of 1:5.6 (0.178) was used for

SCWF-7 than the mass ratio of 0.143 used for SCWF-4. As shown in Figure 18, the visual appearance and microstructure of SCWF-7 is very similar to that of SCWF-4, and, although not quantified, there do not appear to be significantly more salt inclusions formed in SCWF-7.

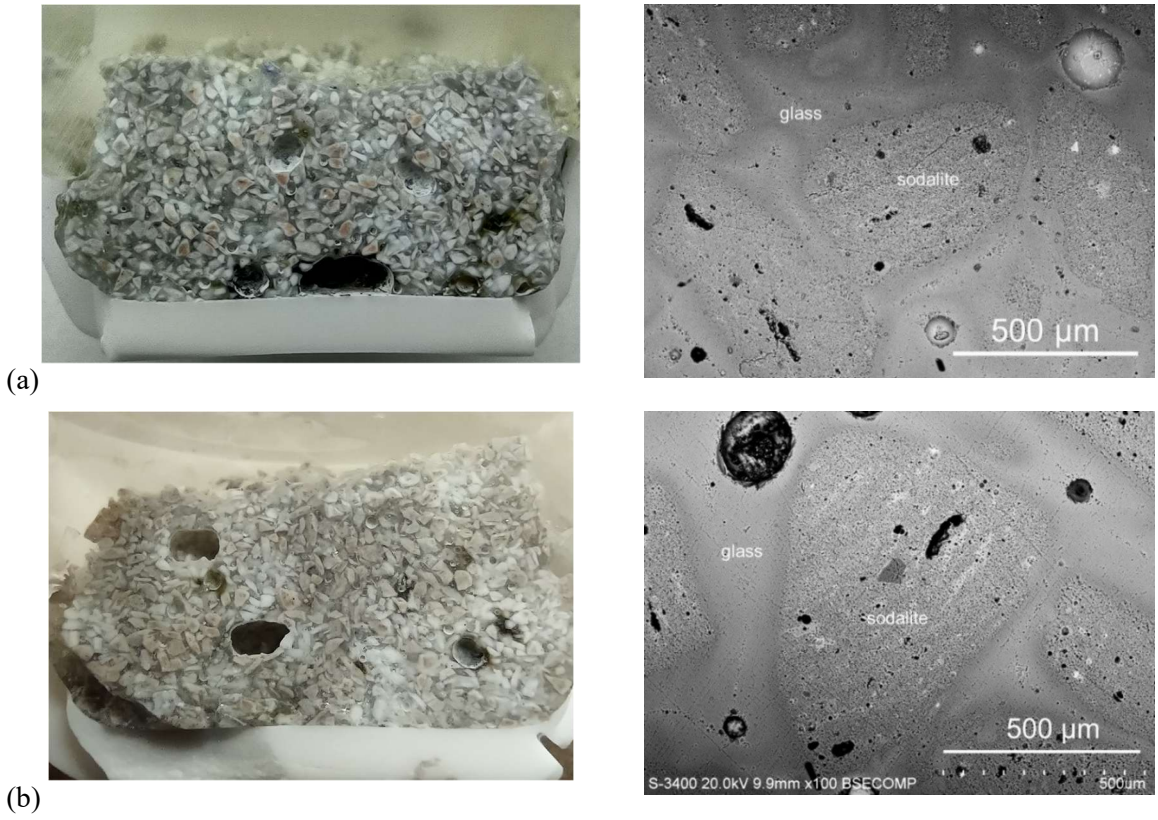

Figure 18. Photograph and microstructure of region (a) of SCWF-7 made with a superstoichiometric salt:Zeolite 4A ratio and (b) SCWF-4 made with a stoichiometric ratio.

Steel Canister Interaction

Material SCWF-8 was made under the same conditions as SCWF-4, except (1) the salt:Zeolite 4A ratio was substoichiometric (0.11 compared to 0.14) and (2) the reagents were contained in a Type 304 stainless steel canister to assess interactions that could occur during processing. The volume of the steel canister was smaller than the volume of the alumina crucibles used to make other SCWF materials, and only about 5 g of reagents was processed compared to about 10 g of reagents processed in the alumina crucibles. Figure 19 shows an optical photograph of the cross-sectioned SCWF-8 canister that had been filled with epoxy. As occurred for materials processed in alumina crucibles, the SCWF material consolidated to ~60% of the volume occupied by the reagents (which had filled the canister to the top), but shrank away from the crucible only slightly. The microstructure of the product material indicates that the steel canister did not inhibit the conversion of Zeolite 4A to sodalite or its encapsulation. The low salt:Zeolite 4A mass ratio used to synthesize SCWF-8 did not noticeably affect the microstructure. Although no core regions of unreacted Zeolite 4A were detected, there appears to be fewer halite inclusions and more pockets of glass within the sodalite domains, such as those located by the arrows in Figure 19b. That could be associated with the fate of excess Zeolite 4A contacted by glass or could be fortuitous.

Figure 19. (a) Optical photograph of cross-sectioned SCWF-8 in steel canister and (b) photomicrograph showing microstructure with regions of glass within sodalite domains.

A photomicrograph and EDS X-ray maps of a typical region of material at the interface with the steel canister are shown in Figure 20. The canister was almost exclusively contacted by the glass phase. The chlorine map shows background levels of chlorine in the glass phase and the steel canister, with some signals from pores that are polishing artifacts. Interaction with the canister resulted in the loss of chromium from near the steel surface and transport of chromium to form a thin band several micrometers within the glass parallel to the interface. Chromium was not detected in EDS spot analysis of binder glass at locations away from the interface with the canister. A few isolated regions of chromium-bearing features are detected further into the bulk that are probably polishing debris. Chromium is mostly retained at the perimeter as the primary corrosion product (~25 at%) having a low iron content (<2 at%). The depth of the chromium depleted region in the steel canister after 2 h at 925 °C is less than 30 µm. These results indicate corrosion of the canister is limited to the oxidation of chromium at surface, but the corrosion rate is sufficiently low (<15 µm/h) that the integrity of the canister is unlikely to degrade significantly during processing at 925 °C. The results of SCWF-8 indicate the use of Type 304 stainless steel canisters will not interfere with the conversion of Zeolite 4A to sodalite to sequester chlorine or consolidation of the product in glass.

3.3 Degradation Behavior

The ASTM C1308 test method has been routinely used to measure the intrinsic dissolution rates of CWF materials under highly dilute conditions (ASTM 2025a). The test is conducted by immersing a specimen with known surface area and gross composition in a large volume of demineralized water to achieve a low specimen surface area-to- solution volume ratio, heating at 90 °C, and completely exchanging the solution with fresh water every 24 hours. Note that the fresh water added during each exchange is not preheated (and had not been preheated in previous tests with other CWF materials), and about one hour is required to

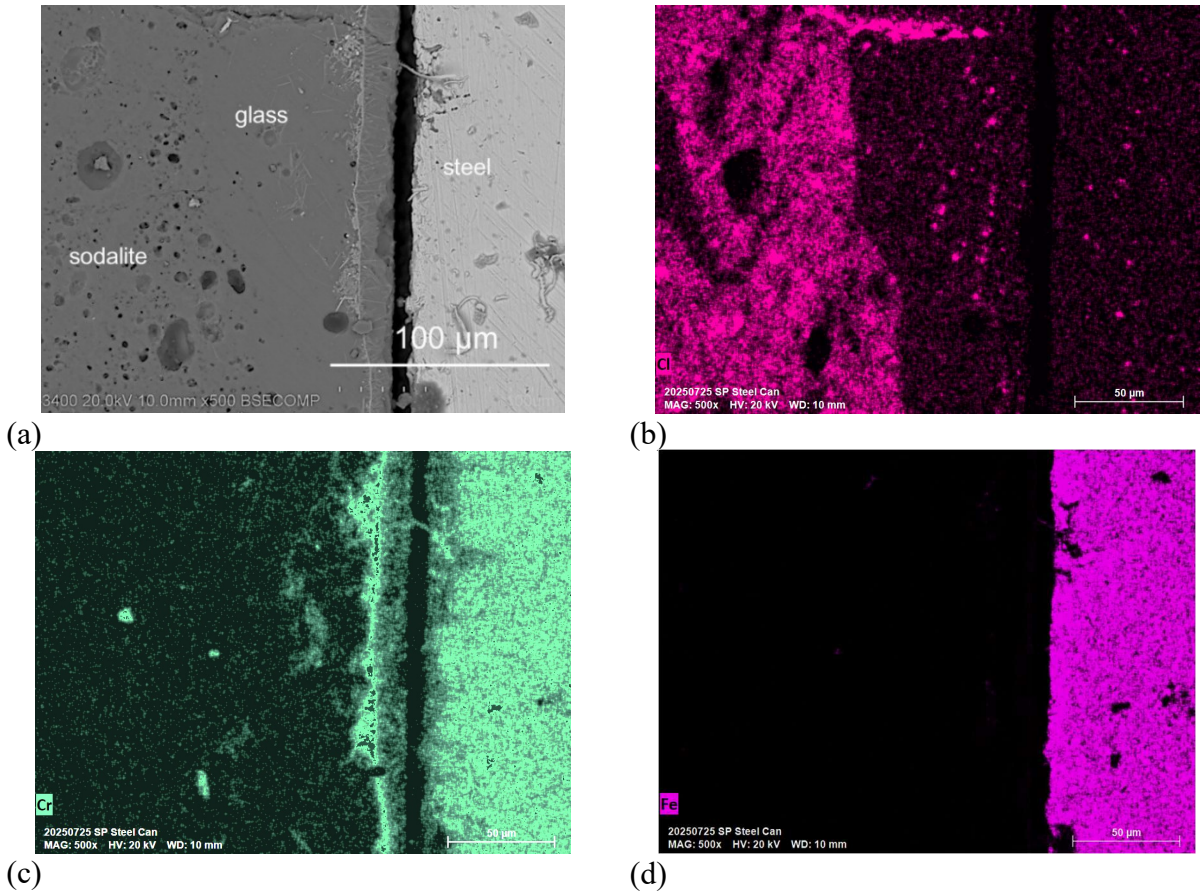

Figure 20. Microstructure of region of SCWF-8 at interface with canister (a) photomicrograph and EDS X-ray maps of (b) chlorine, (c) chromium, and (d) iron.

heat the vessel to 90 °C. The solution concentrations of key elements are measured at each exchange and used to quantify the mass of the specimen dissolved. The slopes of plots of the cumulative releases of key elements over cumulative duration normalized to the specimen surface area and mass fraction of each element in the SCWF material provide a measure of the intrinsic dissolution rate of the material as the average over the last three test intervals. The concentrations measured after the first interval are dominated by dissolution of highly soluble salt inclusions and are affected by sample preparation. The *y*-intercepts of the plots represent the amounts that dissolved rapidly. Concentration measured after the three following intervals are dominated by dissolution of sodalite, binder glass, and any salt inclusions that become exposed during the interval. The average of release rates during the second, third, and fourth intervals are used to represent the intrinsic material durability.

The measured solution concentrations are normalized to the estimated surface area of SCWF-4 exposed at the surface of the polished cross section (the entire mount was immersed) and the element mass fractions calculated from the amounts and compositions of Zeolite 4A, NBS4 glass, and ERX salt used to synthesize the material. Test results are evaluated in terms of the normalized elemental mass loss values calculated for each test interval (i.e., after each solution exchange). The normalized elemental mass loss function NL(i) utilizes the concentration of a soluble element *i* measured in the test solution to represent the mass of the material being tested that had dissolved (in this case, the multiphase SCWF material). The NL(i) values calculated using different species are used to differentiate dissolution of sodalite, glass, and salt phases. The

dissolved mass is normalized to the geometric surface area of the test specimen to provide a value that can be used to compare tests with different specimen areas. Dissolution occurring in each interval of a test series is referred to as the incremental normalized mass loss and is calculated as

$$incremental\ NL(i) = \frac{C(i)_n}{S/_V f(i)}, \quad (2)$$

where $C(i)_n$ is the concentration of species i measured in the test solution during test interval n, S is the geometric surface area of the test specimen, V is the volume of test solution, and $f(i)$ is the mass fraction of species i in the CWF or ACWF material used in the test. Values of NL(i) are presented as g m^{-2} and represent the mass of SCWF material that dissolved during the test interval, not the masses of individual species i that have been released. These values allow for direct comparisons of materials having different compositions (i.e., materials made with different amounts of binder glass, Zeolite 4A, and salt) in tests conducted at different S/V ratios and with different exchange intervals. For the ASTM C1308 tests, the cumulative dissolution occurring through a series of n test intervals is calculated as the sum of the n incremental $NL(i)_n$ values as

$$cumulative\ NL(i) = \sum NL(i)_n = \sum \frac{C(i)_n}{S/_V f(i)}, \quad (3)$$

It is important to remember that the cumulative value determined in a series of intervals in an ASTM C1308 test includes the effect of exchanging the solution with fresh water and does not account for the solution feedback effects of the cumulative solution. It does include the cumulative effect of surface degradation on the exposed areas of constituent phases during each interval, which could increase or decrease during the test.

Figure 21 shows the results of an ASMT C1308 test conducted with the polished cross section of SCWF-4. The y-intercepts of plots of NL(Na), NL(Cs), and NL(K) indicate that an appreciable amount of salt that was exposed at the surface of the specimen dissolved quickly, but the slopes from subsequent intervals indicate the releases of those elements were limited by matrix dissolution thereafter. Figure 21b shows plots of NL(B), NL(Si), and NL(Li) on an expanded scale. The relative slopes of NL(B) and NL(Si) indicate that dissolution of sodalite was slightly more extensive than dissolution of glass. Boron is only present in glass and the release of boron is directly related to the durability of the glass, whereas silicon is released

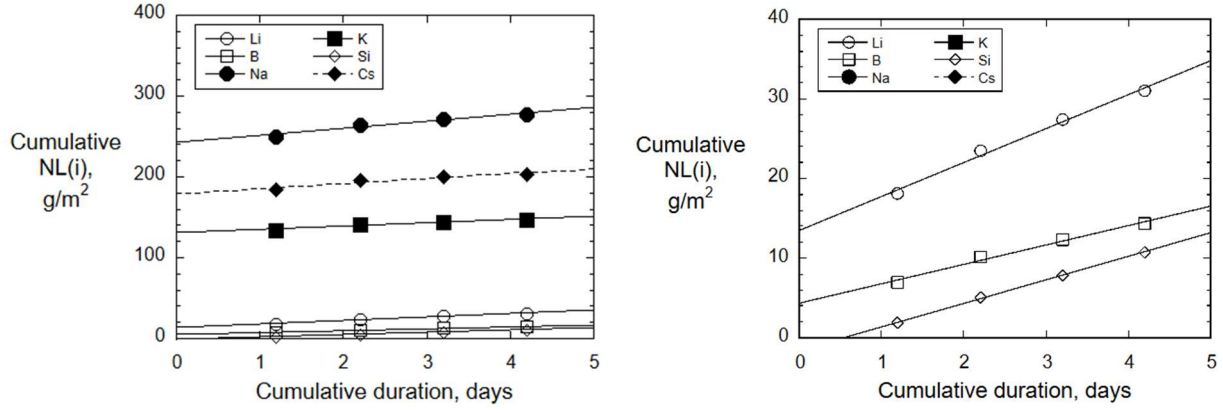

Figure 21. Plots ASTM C1308 test results with SCWF-4 (a) cumulative NL(i) values for lithium, boron, sodium, potassium, silicon and cesium and (b) NL(i) values for lithium, boron, and silicon.

simultaneously from the glass and sodalite. Therefore, the dissolution rate of 2.4 g $m^{-2}d^{-1}$ calculated based on boron only represents dissolution of glass, and the dissolution rate of 2.9 g $m^{-2}d^{-1}$ calculated based on silicon represents the total dissolution of glass and sodalite. Dissolution rates (beyond the first interval) calculated based on lithium, sodium, potassium, and cesium are slightly higher (4.1-8.7 g $m^{-2}d^{-1}$) than the rates calculated based on boron and silicon. The observation that the plot of NL(Li) did not have a high *y*-intercept and had a slope only slightly higher than NL(B) suggests that lithium was primarily released from the glass phase. The dissolution rates of the glass and sodalite phases in SCWF-4 are similar to rates measured for PC CWF materials, such as shown in Figure 22 for material ACWF-N4-11 made with 11% salt loading (Ebert et al. 2017).

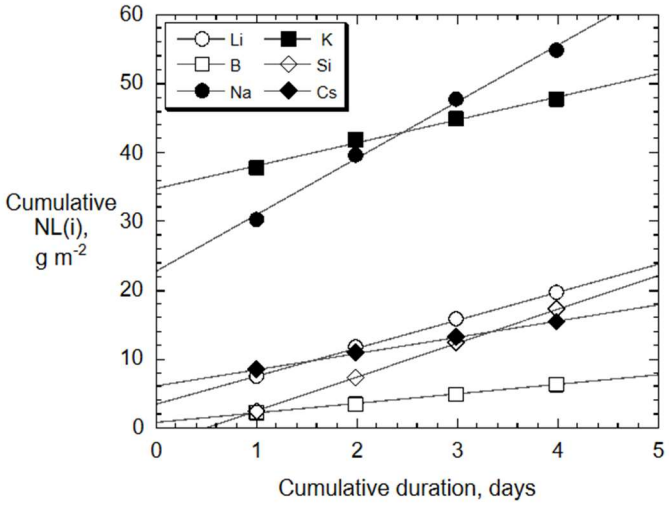

Figure 22. Plot of ASTM C1308 test results for PC material ACWF-N4-11 made with 11% salt loading.

The ASTM C1308 tests with SCWF-4 were continued as static tests (i.e., without exchanging the test solutions with fresh water) to dissolve enough material to detect by using SEM. Figure 23 shows the microstructure of the polished surface before the test and the corroded surface after several weeks of dissolution (different areas of the specimen surface are shown).

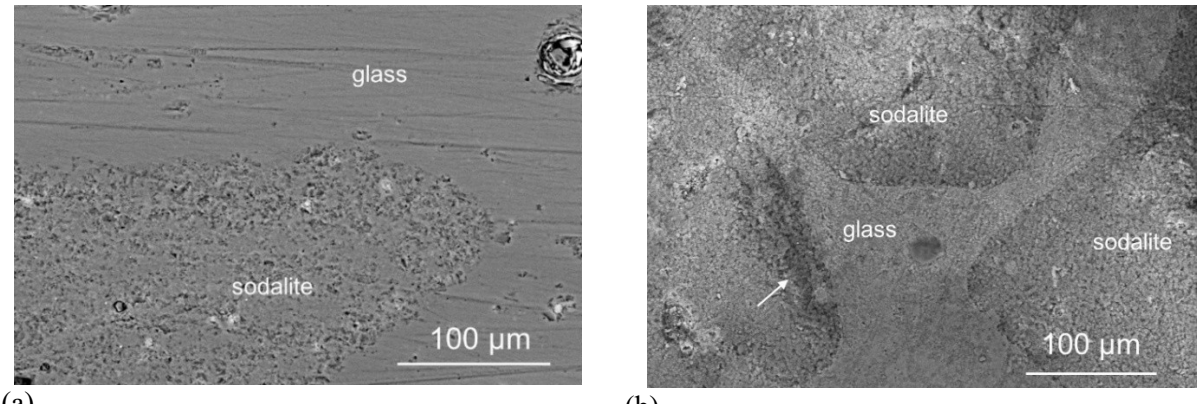

(a) (b)

Figure 23. Photomicrographs of polished SCWF-4 surface (a) before and (b) after immersion test.

The differences are subtle but noticeable. First, the interfaces between sodalite domains and the adjacent glass are sharper and better defined after the test, probably due to preferential dissolution of the sodalite. Some areas of the outer perimeters of sodalite domains have been dissolved, such as the region located by the arrow in Figure 23b. In addition, the reacted surfaces of glass domains appear somewhat geometrically textured, without the mostly directional polishing groves seen on the prepared surface, and glass between sodalite grains in sodalite domains that were apparent prior to the test have dissolved. The extent of dissolution was not sufficiently extensive to warrant generating a cross section to characterize the reacted depth; longer reaction times or higher reaction temperatures would be required.

Note that the dilute conditions maintained during the ASTM C1308 tests remained unsaturated with respect to both sodalite and glass. The higher dissolved silica concentrations that will occur in static solutions generated in a disposal facility will suppress sodalite dissolution while glass dissolution continues. Whereas ASTM C1308 test conditions provide the best measure of intrinsic material durability that is most sensitive to effects of composition and processing conditions, other methods such as ASTM C1285 (ASTM 2025b) provide test conditions that better represent performance in concentrated solutions expected in a disposal system. It is recommended that additional test methods be applied to SCWF materials made in the future.

4. SUMMARY AND RECOMMENDATIONS

The production of small-scale materials using a simplified method demonstrated that directly processing waste salt to generate glass-bonded sodalite CWF at large scale is feasible. The microstructures of materials made with different particle sizes of glass and Zeolite 4A reagents, a range of reagent ratios and water contents, different processing thermal cycles, and crucible materials indicated that in situ generation of sodalite occurred within the molten glass and become microencapsulated in the solidified glass. Residual unreacted Zeolite 4A was only detected in the material SCWF-5 that was made with ~4 mm diameter beads and processed for only two hours to intentionally only partially convert the Zeolite 4A to sodalite in order to gain insights into the process and kinetics. Additional materials can be made using uncrushed smaller beads to further assess the conversion kinetics in future tests.

Formulation of CWF materials must balance the stoichiometry of sodalite generation with encapsulation of sodalite within the glass phase, utilization of sodium in the reagent glass to increase the amount of sodalite generated, and generation of an acceptable amount of halite by-product. Results of this direct processing study suggest the size of Zeolite 4A aggregates should be as small as can be transported effectively in the production system to maximize waste loading and process kinetics. Sizing the binder glass to match the size of Zeolite 4A is expected to facilitate mixing.

The distribution of sodalite domains indicate the reagent salt was uniformly distributed throughout the product volume during processing, even though the salt melting temperature (approximately 370 °C) is significantly lower than the sodalite generation temperature (approximately 850 °C). This suggests the molten salt coated the Zeolite 4A and glass particles and was held until the conversion reaction occurred, and that salt may have become dissolved or dispersed in the molten glass prior to reaction with Zeolite 4A.

The SCWF materials made with Zeolite 4A beads that had not been crushed indicate sodalite is generated as an outer shell by in situ reaction of salt with grains at the outer surface of the Zeolite 4A aggregate that moves inward as molten glass and salt migrate through channels between the zeolite grains. The uniform microstructure throughout cross-sectioned sodalite domains suggests the salt and glass penetrate the zeolite aggregates together, as if the salt is dissolved or dispersed in the glass at the conversion temperature. In contrast to CWF made using the PC method, most small halite inclusions occurred within the sodalite domains whereas larger salt inclusions were distributed in the glass surrounding the sodalite domains. In the CWF materials made using the PC method, the stoichiometric amount of salt was occluded in the Zeolite 4A microstructure prior to processing and only glass penetrated into the Zeolite 4A domains during processing. In these SCWF materials, NaCl must be transported into the Zeolite 4A aggregates along with glass to react and generate sodalite. The microstructures of these SCWF materials indicate that other salt cations (e.g., potassium) remain dissolved in the glass and excess salt remains as inclusions in the glass surrounding the sodalite domains.

The uniformity of the products made with crushed Zeolite 4A suggests much of the salt becomes dissolved into the glass and contacts the zeolite to facilitate conversion. The structure of SCWF-5 material made using uncrushed beads showed that all zeolite grains behind the chlorine penetration front were converted to sodalite, and that glass/salt penetration into the beads was the rate-limiting process. Using crushed Zeolite 4A decreases the distance to which glass/salt must migrate to penetrate to the center of the zeolite domains and shortens the time required to fully process the mixture.

Glass appears to completely wet all the sodalite surfaces at the perimeters and within the sodalite domains, but small voids remain within the sodalite domains. These are more visible in the SCWF materials than in PC CWF materials, although similar amounts of large voids form in both materials. The glass-bonded sodalite waste form is a porous material with mostly closed porosity within the sodalite domains and

throughout the encapsulating glass matrix. Similar porosities occur in materials made using the PC method and by direct processing based on visual examinations. Compacting the materials during processing (e.g., by placing a weight on top) is not expected to increase the density significantly due to the rigidity of the sodalite domains, but this has not been demonstrated. Instead, sizing the Zeolite-4A aggregates for efficient packing and adding the appropriate amount of glass to encapsulate the resulting well-packed sodalite domains is likely an effective approach. Higher processing temperatures will likely increase the density slightly, but at the cost of longer processing times (heating and cooling). In addition, larger SCWF products are expected to densify due to the greater mass than what had occurred during processing the small 10-g laboratory scale products to assess the conversion process.

In the conceptual approach envisioned for large-scale industrial production, molten salt is added (e.g., as a spray) to a mixture of Zeolite 4A and glass of known masses that has been preheated in a stirred mixer or tumbler that is maintained at an elevated temperature. The mixture of Zeolite 4A and glass particles thereby becomes coated with a layer salt before the mixture is loaded into a pre-heated steel canister. The canister is then transferred to a bottom-load furnace and processed.

The methods and engineering approaches to remotely distribute molten salt in the glass/Zeolite 4A mixture, control the relative amounts of reagents, the method and extent of mixing required, and the method to load the mixture into the can remain to be determined. These SCWF materials were synthesized using hand-mixed particles of Zeolite 4A, glass, and solid salt. The design, construction, and testing of lab-scale devices to add molten salt to heated mixtures of Zeolite 4A and glass would inform engineering solutions for large-scale implementation.

In addition to more thoroughly measuring the chemical and physical durability of larger SCWF materials, the thermal stability and heat tolerance should be confirmed. Measurements made to support qualification of PC CWF materials for disposal are expected to be relevant to SCWF materials, but that should be confirmed.

REFERENCES

ASTM (2025a). *Standard Test Method for Accelerated Leach Test for Measuring Contaminant Releases from Solidified Waste*. C1308-21. ASTM-International Annual Book of Standards volume 12.01.

ASTM (2025b). *Standard Test Methods for Determining Chemical Durability of Nuclear, Hazardous, and Mixed Waste Glasses and Multiphase Glass Ceramics: The Product Consistency Test (PCT)*. C1285-21. ASTM-International Annual Book of Standards volume 12.01.

Ebert, W.L. (2005). *Testing to Evaluate the Suitability of Waste Forms Developed for Electrometallurgically Treated Spent Sodium-Bonded Nuclear Fuel for Disposal in the Yucca Mountain Repository*, Argonne National Laboratory report ANL 05/43.

Ebert, W.L., Frank, S.M., and Riley, B.J. (2016). *Designing Advanced Ceramic Waste Forms for Electrochemical Processing Salt Waste*. DOE NE report FCRD-MRWFD-2016-000038. Argonne National Laboratory.

Ebert, W.L., Riley, B.J., and Frank, S.M. (2017). *Test Plan for Salt Treatment and Waste Form Development*. DOE NE report NTRD-MRWFD-2017-000191. Argonne National Laboratory.

Ebert, W.L. (2024). *Simplifying Ceramic Waste Form Processing*. Argonne report ANL/CFCT-24/7. Argonne National Laboratory.

Priebe & Bateman (2008) "*The Ceramic Waste Form Process at Idaho National Laboratory." Nuclear Technology, 162:2 pp 199-207.*